

UNIVERSAL MEMS PLATFORMS FOR PASSIVE RF COMPONENTS: SUSPENDED INDUCTORS AND VARIABLE CAPACITORS

L. Fan, R. T. Chen, A. Nespola, and M. C. Wu

Department of Electrical Engineering
University of California, Los Angeles
66-147D Engineering IV Building
Los Angeles, CA 90095-1594
Tel: (310) 825-6859 Fax: (310) 825-6954
Email: wu@icsl.ucla.edu

ABSTRACT

We propose a universal MEMS technology platform for fabricating integrable passive components for radio frequency (RF) integrated circuits. This platform is based on a novel surface-micromachined Micro-Elevator by Self-Assembly (MESA) technique. Both high-Q inductors and variable capacitors can be realized by the MESA technology. A surface-micromachined spiral inductor that is raised by 250 μm above the Si substrate has been experimentally demonstrated. The suspended inductor has less parasitic capacitance and substrate loss, and higher quality (Q) value and resonant frequency. The inductance of a 12.5-turn inductor is measured to be 24 nH. The results show that the self-assembled passive RF elements are suitable for monolithic integration.

INTRODUCTION

Integrable passive radio frequency (RF) components such as inductors and variable capacitors are of great interest to RF integrated circuits. Inductors and transformers offer additional capability in RF circuits since they enable the use of passive filtering, impedance matching, inductive loading, and other techniques that are not available at the integrated circuit level. The advances in today's high-speed transistors have made it possible to integrate wireless communication circuits monolithically. However, the passive RF components remain bulky and cannot be integrated.

The MicroElectroMechanical Systems (MEMS) technology offers a powerful tool to fabricate integrated passive RF components. Miniaturization of conventional coil inductors on substrates has been demonstrated using electroplating and planarization

techniques [1-7]. High Q inductors can be built that way, however, they have low resonant frequencies and are not compatible with complementary metal-oxide-semiconductor (CMOS) technique. They are typically used in power and DC (or low frequency) applications. Planar spiral inductors are more commonly used in RF integrated circuits [8]. The parasitic capacitance and the finite resistivity of silicon substrates limit the value of achievable Q. Selective removal of the Si substrate underneath the spiral inductors by wet etching [9-11] have been shown to be very effective in increasing the inductors' Q and resonant frequency. However, relatively large openings in the cavities are required. Recently, dry etching (SF_6) has been shown to suspend inductors on silicon-on-insulator (SOI) wafers [12].

Instead of suspending the inductors by selective removal of substrate, it is also possible to achieve high Q by raising the inductor spirals above the silicon substrate. Previously, we have proposed and demonstrated a novel Micro-Elevator by Self-Assembly (MESA) technique, which can raise a platform to several hundred micrometers above the Si surface. The MESA actuators have been utilized to implement micro XYZ stages and to manipulate a micro ball lens [13,14]. In this paper, we will describe a new technique to realize high Q inductor by employing the MESA structures. The MESA structure can also be applied to fabricate variable capacitors. Though the fabrication of variable capacitors is less challenging, and many micromechanical variable capacitors have been demonstrated [15,16], the fabrication technique is usually different from that for inductors or standard CMOS processes. The different fabrication processes required for each RF component makes it difficult to monolithically integrate these components on the same

substrate. Therefore, a unified fabrication technology for all passive RF components is highly desired.

PRINCIPLE AND DESIGN

The Micro-Elevator by Self-Assembly (MESA) structure is illustrated in Fig. 1. It is made by the surface-micromachining technique, and consists of three parts: the center platform (shown as inductor coil here), the side-support plates, and the microactuator plates. These surface-micromachined plates are connected by the microhinges [17]. The MESA platform can be raised above the Si surface by biasing the two actuator arrays to move towards each other at the same speed. To ensure the planarity of the MESA platform, there are two approaches: (1) employ side-support plates on all four sides of the platform [14], and (2) use additional springs to properly balance the force on the platform.

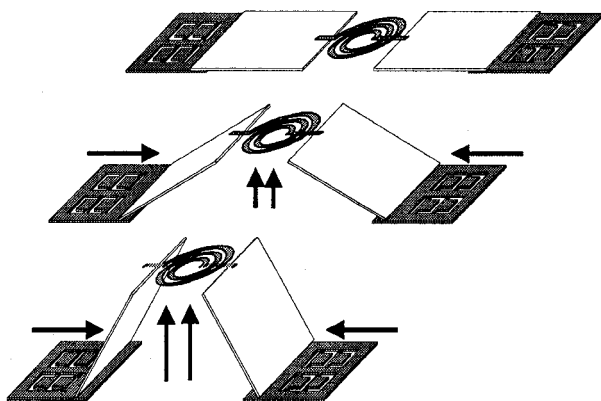


Fig. 1: Schematic of MESA structure.

The MESA technology is unique because it offers a new approach to achieve large out-of-plane structures without employing thick sacrificial layers or LIGA processes. It is completely self-assembled. Moreover, the height of the platform is adjustable by controlling in-plane actuators. MESA platforms as high as 250 μm and as large as 5 mm x 5 mm have been experimentally demonstrated. In principle, the height of the MESA structure is determined by the length of the side-support plate. Platforms higher than 1 mm should be feasible. Therefore, the MESA technology is ideal to implement suspended inductors and possibly transformers.

The schematic diagram of the suspended inductor realized by the MESA technology is shown in Fig. 1. The spiral inductor is patterned on the center platform of the MESA structure. The microactuators move toward each other to lift the inductor vertically and suspend it above the substrate. Low parasitic capacitance and low substrate loss can be achieved

without etching the substrate. The resonant frequency is also increased.

The MESA structure can also be applied to fabricate variable capacitors. The capacitance of a parallel plate capacitor can be varied by changing the gap spacing or the overlap area between the plates. The variable-gap capacitor is realized in a similar fashion as the suspended inductor. The inductor coil is replaced by a solid electrode and placed above a fixed electrode. The two electrodes form a parallel plate capacitor. The capacitance can be varied by changing the height of the suspended electrode. Figure 2(a) shows the schematic diagram of a variable capacitor using the MESA technology.

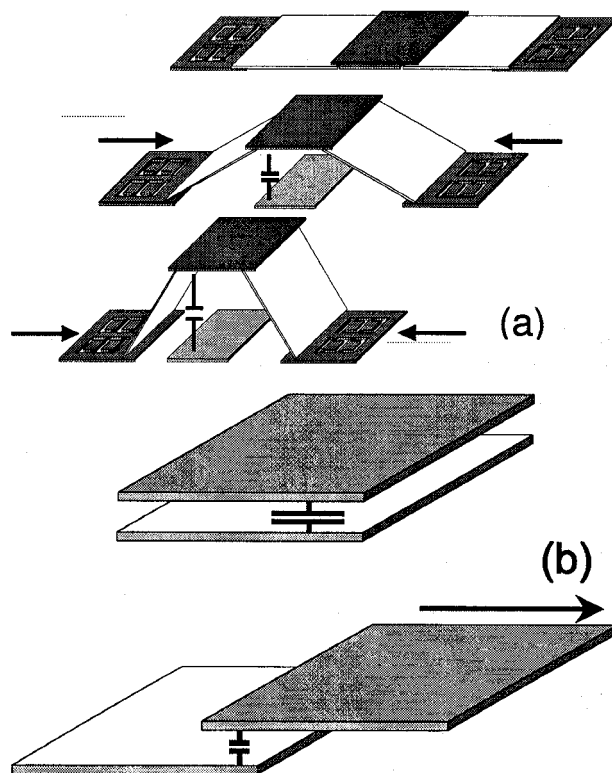


Fig. 2: Variable capacitor realized by the MESA technology with (a) variable gap spacing and (b) variable overlap area.

Since the capacitance is inversely proportional to the gap spacing, the capacitance decreases very rapidly as the gap increases. This may limit the tuning range. Another type of variable capacitor varies the overlap area of the parallel plates, as illustrated in Fig. 2(b). This can be realized by moving the MESA structure in the lateral direction, which has been demonstrated in our previous report on micro-XYZ stage [14]. Larger tuning can be achieved.

FABRICATION

The three-dimensional MESA structure is fabricated using the three-polysilicon-layer surface-micromachining foundry offered by the Microelectronics Center of North Carolina (MCNC). The inductor coil is patterned on the second polysilicon layer and coated with 0.5- μm -thick gold to reduce its resistance. The structures are completely self-assembled by the integrated microactuators. In principle, any actuator with large linear travel range and bi-directional motion can be used to assemble MESA. We have employed scratch drive actuator (SDA) array [18] because it is compact, easily integrable with MESA structures, has large force, fine step resolution, and virtually unlimited travel range.

To attain the precision required for the MESA structure, improved microhinges, called *polarity hinges*, have been used to join the platform, side-support plates, and microactuator plates. The MESA platform is raised above the Si surface by pushing the two actuator arrays towards the center. The principle is similar to that of a buckle beam. However, with regular hinges, the platform can buckle either upward or downward. To have a unique direction of motion, polarity hinges are used to join the polysilicon plates. Similar to the conventional scissors hinges [17], the polarity hinges allow the joined plates to bend only in one predetermined direction (either upwards or downwards). However, unlike scissors hinges, the uncertainty of the lateral gap between polysilicon plates has been greatly reduced from 10 μm to 2 μm . Tight control of the lateral gap is critical to the successful operation of MESA. Details of the polarity hinge design can be found in [14].

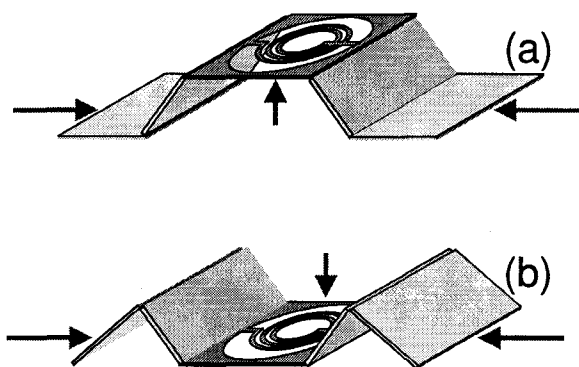


Fig. 3: Without the polarity hinges, the center platform could buckle either (a) upward or (b) downward.

Another issue of the microhinges for applications in RF circuits is its high contact resistance between the hinge parts, which results in low Q values. To counter this problem, we have modified the microhinges to include torsion beams. The torsion beams eliminate the contact resistance, however, they are subject to large lateral movement. When microhinges are used in conjunction with torsion hinges, the microhinges limit the lateral movement while the torsion beams improve the resistance.

The inductors are electrically contacted through the side-support plates. For mechanical support, the suspended inductor is attached to a polysilicon frame that is hinged to the side-support plates. To prevent the inductor from being shorted by the frame, which is made of conductive polysilicon material, hard-baked photoresist is used to connect one lead of the inductor to the rest of the structure. Before the structure is released, the photoresist is patterned between the two isolated leads of the inductor. The photoresist is hard baked to ensure mechanical stiffness. After release, the platform is rigid and the inductor leads are isolated. The inner end of the coil is connected to the isolated side-support plate by an air bridge patterned on the first polysilicon layer. The scanning electron micrograph (SEM) of the suspended inductor is shown in Fig. 4.

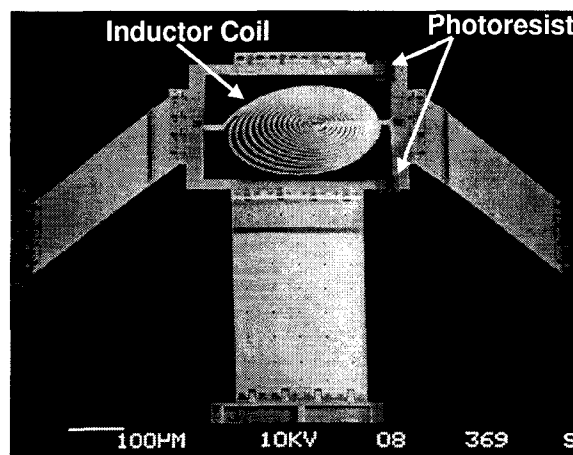


Fig. 4: Scanning electron micrograph of the suspended inductor supported by the MESA structure.

SIMULATION AND MEASUREMENTS

Inductors

The effect of suspended inductor is investigated theoretically and experimentally. A finite-element electromagnetic field simulator (HFSS) has been employed to calculate the scattering parameters of a suspended inductor and an inductor on the substrate. To

reduce the simulation time, the simulated inductors has only 1.5 turns. The coils are made of a 0.5- μm -thick gold film. The outer and inner ring radii are 150 μm and 120 μm , respectively. The conductor is 4 μm wide and the spacing between the rings is 4 μm . The suspended inductor is 250 μm above the substrate. Suspending the inductor above the substrate results in an increase in the self-resonant frequency from 25 GHz to 48 GHz, as shown in Fig. 5.

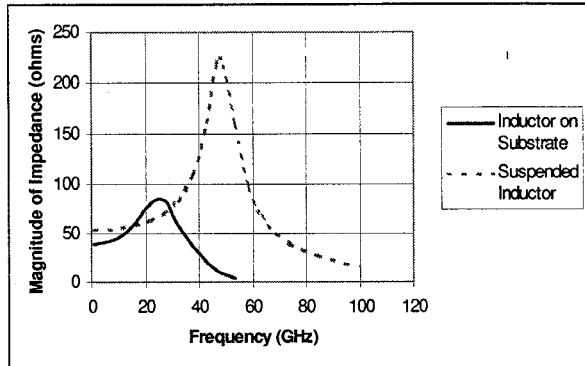


Fig. 5: Simulation of the magnitude of impedance versus frequency for the 1.5 turns suspended inductor and the inductor on substrate.

Experimentally, the inductance of an inductor suspended by the MESA structure has been measured by an RF gain-phase analyzer (HP 4194A). The inductor under test has 12.5 turns, and the outer diameter of the spiral is 137 μm . The inductor is patterned on the second polysilicon layer, which is 1.5 μm thick, and coated with 0.5- μm -thick gold film to reduce its resistivity. The resonant frequency increases from 1.8 GHz to 6.6 GHz. The inductance is measured to be 24 nH, which agrees reasonably well with the calculated value of 28 nH.

Capacitors

The variable capacitor is realized in a similar fashion as the suspended inductor. Figure 6 shows the SEM micrograph of the tunable capacitor realized by variable gap spacing. The 250 \times 250- μm^2 polysilicon plate is raised above the substrate by four 300- μm -long side support plates. The capacitance is varied by changing the height of the suspended electrode. The gap spacing is determined by the lateral movement of the scratch drive actuator arrays. Since the capacitance is inversely proportional to the gap spacing, the capacitance decreases rapidly from 500 fF to 20 fF when the suspended electrode is raised from substrate to a height of 250 μm . Since the capacitance change is not linearly proportional to the displacement, it could be difficult to achieve fine tuning adjustment. This can be improved by using MESA structure with variable overlap area as

illustrated in Fig. 2(b). Large tuning range and linear tuning can be achieved.

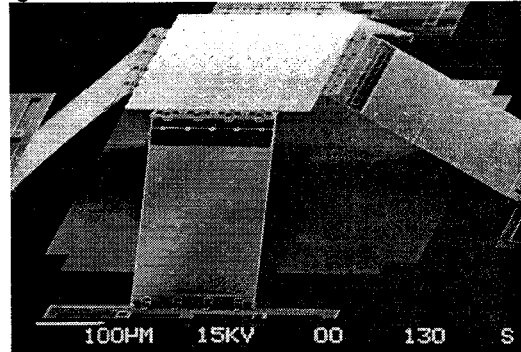


Fig. 6: Scanning electron micrograph of the suspended capacitor supported by the MESA structure.

FUTURE WORK

The suspended inductor shown in Fig. 4 is connected by hard-baked photoresist to achieve electric isolation and enhance its mechanical strength during assembly. An alternative structure is shown in Fig. 7. One end of the inductor coil is pulled up by the micro-elevator while the other end is attached to the ground electrode. This inductor coil can be completely self-assembled without using any hard-baked photoresist. This configuration has slightly higher parasitic capacitance. Potentially, a tunable inductor can be realized by monolithically integrating the coil with a permalloy core.

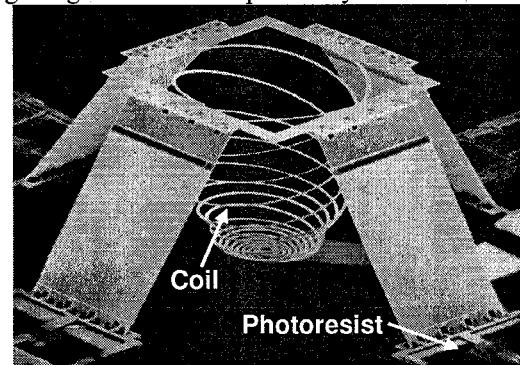


Fig. 7: Scanning electron micrograph of the suspended inductor supported by the MESA structure.

We are currently designing new three-dimensional structures that may further enhance the performance of suspended inductors. Some of our designs include vertical inductors that assembled vertically to the substrate surface. These inductors may have even lower parasitic capacitance and substrate loss. With two vertical inductors assembled adjacent to each other, as shown in Fig. 8, transformers or cascaded inductor array can be realized.

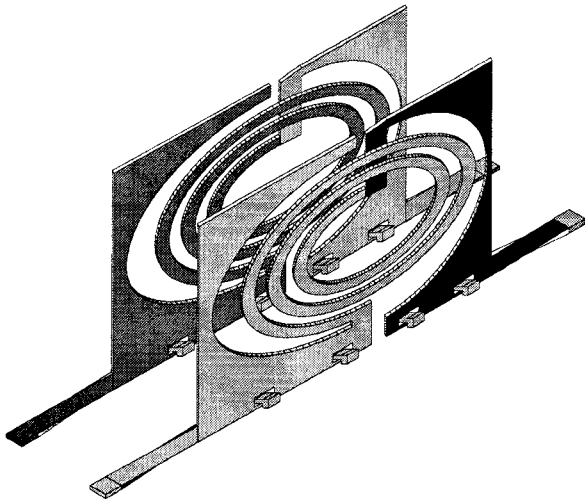


Fig. 8: Transformer realized by two vertical inductors assembled adjacent to each other.

CONCLUSION

We have proposed and demonstrated a new universal MEMS platform for RF components utilizing the MESA technology. Self-assembled suspended inductors and variable capacitors have been demonstrated for the first time using the standard surface-micromachining technology. The performance of the inductor has been improved over the conventional surface inductors without using bulk etching.

ACKNOWLEDGEMENTS

The authors would like to thank Tai Chau and Dennis Tong for technical assistance. This project is supported in part by DARPA and the Packard Foundation.

REFERENCES

- [1] M. Kimura and J. Hayasaki, "Characteristics and simulations of the planar multi-layer spiral coil and the miniature opto-electric transformer," *IEEE Transactions on Magnetics*, vol. 29, pp. 3216 – 3218, 1993.
- [2] C. R. Sullivan and S. R. Sanders "Microfabrication of transformers and inductors for high frequency power conversion," *IEEE Power Electronics Specialists Conference*, pp. 33 – 41, 1993.
- [3] C. H. Ahn and M. G. Allen, "A comparison of two micromachined inductors (bar-type and meander type) for fully integrated boost DC/DC power converters", *IEEE Transactions on Power Electronics*, vol. 11, pp. 239 – 245, 1996.
- [4] J. Y. Park and M. G. Allen, "A comparison of micromachined inductors with different magnetic core materials", *46th Electronic Components Technology Conference*, pp. 375 – 381, 1996.
- [5] D. J. Sadler, W. Zhang C. H. Ahn, H. J. Kim and S. H. Han, "Micromachined semi-encapsulated spiral inductors for micro electro mechanical systems (mems) applications," *IEEE Transactions on Magnetics*, vol. 33, pp. 3319 – 3321, 1997.
- [6] J. A. Von Arx and K. Najafi, "On-chip coils with integrated cores for remote inductive powering of integrated microsystems," *IEEE Transducers*, pp. 999-1002, 1997.
- [7] J. A. Rogers, R. J. Jackman and G. M. Whitesides, "Constructing single and multiple-helical microcoils and characterizing their performance as components of microinductors and microelectromagnets", *Journal of Microelectromechanical Systems*, pp. 184 – 191, 1997.
- [8] N. M. Nguyen and R.G. Meyer, "Si IC-compatible inductors and LC passive filters," *IEEE J. Solid-State Circuits*, vol. 25, pp. 1028-1031, 1990.
- [9] J.Y.-C. Chang, A. A. Abidi and M. Gaitan, "Large suspended inductors on silicon and their use in a 2- μ m CMOS RF Amplifier", *IEEE Electron Device Letters*, vol. 14, no. 5, pp. 246-248, 1993.
- [10] C.-Y. Chi, G. M. Rebeiz, "Planar microwave and millimeter-wave lumped elements and coupled-line filters using micro-machining techniques," *IEEE Transactions on Microwave Theory and Techniques*, vol. 43, no. 4, pp. 730-738, 1995.
- [11] Y. Sun, H. van Zeijl, J. L. Tauritz and R. G. F. Baets, "Suspended membrane inductors and capacitors for application in silicon MMIC's," *IEEE Microwave and Millimeter-Wave Monolithic Circuits Symposium*, pp. 99-102, 1996.
- [12] D. Hisamoto, S. Tanaka, T. Tanimoto, Y. Nakamura and S. Kimura, "Silicon RF devices fabricated by ULSI processes featuring 0.1 μ m SOI-CMOS and suspended inductors," *Symposium on VLSI Technology Digest of Technical Papers*, pp. 104-105, 1996.
- [13] L. Fan and M. C. Wu, "Self-assembled micro-XYZ stage with micro-ball lens for optical scanning and alignment," *International Conference on Optical MEMS and Their Applications*, pp. 45-49, 1997.
- [14] L. Fan, M. C. Wu, K. D. Choquette and M. H. Crawford, " Self-assembled microactuated XYZ stages for optical scanning and alignment," *IEEE Transducers*, pp. 319-322, 1997.
- [15] K. A. Shaw, Z. L. Zhang, N. C. MacDonald, "SCREAM I: a single mask, single-crystal silicon, reactive ion etching process for microelectromechanical structures," *Sensors and Actuators A*, vol. 40, no. 1, pp. 63-70, 1994.
- [16] A. A. Ayon, N. J. Koliass and N. C. MacDonald, "Tunable, micromachined parallel-plate transmission lines," *IEEE/Cornell Conference on Advanced Concepts in High Speed Semiconductor Devices and Circuits*, pp. 201-208, 1995.
- [17] K. S. J. Pister, M. W. Judy, S. R. Burgett, and R. S. Fearing, "Microfabricated hinges," *Sensors and Actuators A-Physical*, vol., 33, no. 3, pp. 249, 1992.
- [18] T. Akiyama and H. Fujita, "A quantitative analysis of scratch drive actuator using buckling motion," *IEEE Micro Electro Mechanical Systems*, pp. 310-315, 1995.